

***In-situ* x-ray absorption fine structure and x-ray diffraction studies of hydrogen intercalation in tungsten oxides**

J. Purans and A. Kuzmin

Institute of Solid State Physics, University of Latvia, LV-1063 Riga, Latvia

C. Guéry

Laboratoire de Réactivité et de Chimie des Solides, Université de Picardie, F-80039 Amiens, France

ABSTRACT

We present *in-situ* x-ray absorption fine structure (XAFS) (at the W L₃-edge) and x-ray diffraction (XRD) studies of hydrogen intercalation into stable monoclinic (m-WO₃) and metastable hexagonal (h-WO₃) and cubic (c-WO₃) phases of tungsten oxide. The analysis of XAFS and XRD data allowed us to reconstruct the local environment around tungsten ions in the first coordination shell. The obtained results are compared with the existing structural models.

Keywords: XAFS, XRD, tungsten oxides, structure, hydrogen intercalation

1. INTRODUCTION

The stable monoclinic (m-WO₃) and the metastable hexagonal (h-WO₃) and cubic (c-WO₃) phases of tungsten oxide exhibit phase transitions of different type [1,2], which can be caused by a change of temperature, stoichiometry, pressure or tungsten valency upon hydrogen intercalation. These phase transitions lead to the modifications of the local and long range atomic orders as well as of the electronic structure of the oxides.

The hydrogen intercalation into m-WO₃ and h-WO₃ has been studied in detail by many methods [1-4]. The x-ray diffraction (XRD) and neutron diffraction measurements have been performed on the tungsten bronzes H_xWO₃ in the range from 0 to 0.6 started from m-WO₃ [4] and h-WO₃ [1]. However, to our knowledge, the hydrogen intercalation in c-WO₃ has not been studied previously.

The goal of this work is to study the local and long range structural changes occurring in the WO₃ oxides upon hydrogen intercalation. Here we present preliminary results on stable m-WO₃ and metastable h-WO₃ and c-WO₃ phases of tungsten trioxide.

2. EXPERIMENTAL AND DATA ANALYSIS

The metastable h-WO₃, c-WO₃ and the stable m-WO₃ tungsten oxides were produced by dehydration of hydrate precursors. The h-WO₃ was prepared by dehydration of WO₃·1/3H₂O at 280°C for about 72 hours under an air flow. On the other hand, c-WO₃ and m-WO₃ were prepared by dehydration of the monohydrate WO₃·H₂O respectively at 235°C for 25 min and at 350°C for several days.

The tungsten oxide bronzes H_xWO₃ were prepared by reaction of molecular hydrogen on a platinized oxide by spillover effect. The bronzes, for x-ray diffraction measurements, were produced by allowing a hydrogen flow to pass through the sample in an air-free atmosphere. The intercalation levels were determined by chemical analysis. The m-WO₃, h-WO₃ and c-WO₃ tungsten oxides were intercalated at room temperature up to about x=0.35.

The x-ray diffraction measurements have been performed at room temperature on a x-ray multichannel Inel diffractometer using the capillary configuration. A Cu K_{α1} radiation from x-ray tube operated at output 20-30 mA and U=40 kV has been used. The XRD measurements have been performed at several intercalation levels up to saturation according to experimental conditions. The refinements of the corresponding cell parameters have been made with a least-squares fit program.

Experimental x-ray absorption fine structure (XAFS) spectra of the W L₃-edge were recorded in transmission mode at the LURE DCI storage ring on the EXAFS-3 beamline located at the bending magnet. The storage ring DCI operated at the energy 1.85 GeV and the maximum stored current 312 mA. A standard transmission scheme with a Si(311) double-

crystal monochromator and two ion chambers containing argon gas was used, and the data were recorded during one injection of the storage ring with a spacing of 2 eV. The samples for x-ray absorption measurements were platinized tungsten oxides mixed with boron nitride powder. The mixture was placed in a closed boron nitride cell mounted in a chamber. The sample had a thickness x giving the value of the x-ray absorption edge jump $\Delta\mu x \approx 1.4$. The hydrogen was intercalated *in-situ* by allowing a hydrogen flow to pass through the sample at room temperature. The XAFS measurements (see Fig. 1) were performed at several intercalation levels up to saturation according to experimental conditions as in XRD experiments.

The XAFS spectra were treated and fitted using the EDA software package [5] (see [6] for details). The theoretical backscattering amplitudes and phases were calculated by the FEFF code and verified before [6]. The origin of the peaks in the Fourier transforms (FT) of the XAFS signals was described by us previously [6-7]. Four main peaks located at 0.6-2.2 Å, 2.2-3.1 Å, 3.35-4.05 Å and 4.4-5.5 Å are present in the FT's of experimental XAFS spectra (see Fig. 1).

The XAFS signals of the first peaks were singled out by the back FT procedure and were utilized in further analysis. The first peak is well isolated and its contribution was singled out by the back-FT in the range 0.8-2.2 Å. The experimental first shell XAFS signals were fitted in the range 2.5-14 Å⁻¹ using two different models: (1) multi-shell model within harmonic or anharmonic (cumulant) approximations and (2) model-independent approach [5] based on the general XAFS model (see [8] for details). The multi-shell model allows one to obtain a set of structural parameters as coordination numbers (N), interatomic distances (R) and the Debye-Waller (DW) factors (s^2). The quantitative analysis of the second, third and fourth peaks in the FT's, complicated by the presence of strong multiple-scattering contributions and many body correlation effects, is in progress and will be published in a forthcoming paper.

3. RESULTS AND DISCUSSION

The h-WO₃ and m-WO₃ are well crystallised and show sharp XRD peaks. The lattice parameters of hexagonal ($a=7.298(2)$ Å, $c=7.798(3)$ Å) and monoclinic ($a=7.284(2)$ Å, $b=7.507(5)$ Å, $c=7.673(7)$ Å, $\beta=90.62^\circ$) phases are in good agreement with the previous data [1-4]. At the same time, c-WO₃ has broad XRD peaks which correspond to simple cubic XRD pattern ($a=3.704$ Å). The measurements of the intercalated m-WO₃ at $x=0.23$ and $x=0.35$ show two different tetragonal phases with tetragonal cell parameters at $x=0.23$: $a=5.238(2)$ Å and $c=3.891(4)$ Å ($Z=2$) and at $x=0.35$: $a=3.764(9)$ Å and $c=3.732(8)$ Å ($Z=1$) in agreement with the literature [1,4]. The intercalation of hydrogen in h-WO₃ leads to a change of the cell parameters to $a=7.364(0)$ Å and $c=7.580(1)$ Å at $x=0.35$ that agrees with the previous observations [1,4]. On the contrary, the hydrogen intercalation in c-WO₃ leads to a very small increase of the cell parameter from $a=3.70(4)$ Å at $x=0.0$ to $a=3.74(8)$ Å at $x=0.35$.

The experimental XAFS signals and their FT's for non-intercalated and intercalated compounds are shown in Fig. 1. The peaks up to 6 Å in the FT's of intercalated m-WO₃ and h-WO₃ are significantly modified by the hydrogen intercalation, while only small changes are observed in the FT of the intercalated c-WO₃. The first peak corresponds to single-scattering processes at six oxygen (O₁) atoms forming the distorted octahedron of the first coordination shell at the distances $R(W-O_1)=1.7-2.3$ Å. The second peak is attributed mainly to multiple-scattering processes within the first shell of the WO₆ octahedra. The third peak corresponds mainly to scattering from the second shell formed by tungsten (W₂) atoms $R(W-W_2)=3.6-3.9$ Å: its amplitude is significantly influenced by the strong focusing effect due to the oxygen atoms of the first shell and depends on the tilting W-O-W₂ angle. Note that oxygens (O₃), located in the third coordination shell, form a broad distribution of the distances $R(W-O_3)=3.7-4.5$ Å with a maximum near 4.2 Å (for example, 24 oxygen in c-WO₃, are located at 4.2 Å), however they also give some contribution to the third peak. The fourth peak corresponds mainly to the single-scattering signal from tungstens W₄ (for example, in c-WO₃ 12 (W₄) atoms are at ~ 5.3 Å and 30 oxygens (O₅) of the fifth shell at ~ 5.6 Å).

The experimental XAFS signals of the first shell were simulated by two approaches mentioned above in section 2. Some multi-shell models (Table 1), based on the XRD structural data, were used to obtain the values of N , R and s^2 . The coordination numbers N were fixed at some numbers depending on how the interatomic W-O distances, given by XRD, were grouped. The quantities R and s^2 were used as fitting parameters. The model-independent approach [5] was used to reconstruct the total first-shell radial distribution functions (RDF) (Fig. 2).

In m-WO₃ there are two non-equivalent types of WO₆ octahedra which contain, from XRD data [3], twelve different W-O distances within the first shell. Therefore to compare XRD and XAFS data one needs to group them in some way (Table 1). Two models of the RDF were tested: the first one is consisting of two groups of 3 oxygen atoms in each, while the second one is composed of three groups of 2 oxygen atoms each (Table 1). The first-shell RDF in m-WO₃ (Fig. 2) has a broad distribution of distances from ~ 1.7 to ~ 2.3 Å [6] and is splitted into two peaks centered at ~ 1.75 and ~ 2.1 Å. The

three-shells fit, corresponding to the model of three groups of two oxygen atoms in each (the model 2:2:2), gives the W-O distances equal to 1.77, 1.90 and 2.14 Å. The shortest bonds have smaller DW factor values due to the fact that the first peak at ~1.75 Å is sharp. The longest bonds have larger DW factors so that the second peak at ~2.1 Å is broadened. Besides, it was found that within the three-shells model, the middle bonds at the center of the distribution have a very large DW factor, $s^2=0.0084 \text{ \AA}^2$ (Table 1). This can explain why the total RDF contains only two main maxima at 1.75 and 2.1 Å (Fig. 2).

As in m-WO₃, also in h-WO₃ two models containing two (4:2) and three (2:2:2) groups of oxygen atoms were tested. The best fitted result for the three-shells model (the W-O distances are equal to 1.78, 1.94 and 2.15 Å) gives better agreement than the two-shells model (see the values of ϵ in Table 1). Within the three-shells model, the middle and long bonds have larger DW factors and therefore the central and last peaks of RDF's are more broadened. The obtained data are in disagreement with the XRD structural model from [1] (two W-O subshells) and are in better agreement with XRD data in [9]. Note that in the latter model, the WO₆ octahedra are very distorted with three types of W-O distances. In the hexagonal plane there are two short ($R=1.75$ (II) or 1.80 Å (I)) and two long W-O bonds (2.04 (II) or 2.19 Å (I)). Also between the layers there are short (1.80 Å) and long (2.13 (I) or 2.18 Å (II)) W-O bonds.

In intercalated m- and h-WO₃ oxides, the RDF's (Fig. 2) differ essentially from the two peaks RDF's of non-intercalated compounds. The three-shells fit and cumulant model of the intercalated H_xWO₃ (m-WO₃) data give one broad asymmetric Gaussian distribution. The intercalated h-WO₃ shows a similar shape with a maximum at 1.8 Å and a shoulder at 2.1 Å. The three-shells fit (2:2:2) of the intercalated h-WO₃ data gives better results and three groups of distances at 1.81, 1.89 and 2.01 Å are obtained. Thus, the local distortion of the WO₆ octahedra decreases progressively upon hydrogen insertion.

The first-shell RDF's for c-WO₃ and H_x(c-WO₃) have broad asymmetric distributions of distances from 1.75 to 2.25 Å with a peak at ~1.85 Å and the average W-O distances $\langle R \rangle = 1.896$ and 1.890 Å, respectively. The one-shell fit with four cumulants and model-independent approach [5] gives one asymmetric Gaussian peak (Fig. 2). The XRD shows (Table 1) that c-WO₃ and H_x(c-WO₃) have only one type of regular WO₆ octahedron with six oxygen atoms at 1.852 and 1.874 Å, respectively. During hydrogen intercalation in c-WO₃, we have observed by XAFS only a small decrease of the W-O distance in the first coordination shell and an increase of the lattice parameter by 0.04 Å (XRD data). This suggests that in c-WO₃ the W-O-W tilting angle increases upon hydrogen intercalation.

4. ACKNOWLEDGMENTS

The authors are grateful to Prof. H. Dexpert, Dr. S. Benazeth, Dr. Ph. Parent and to the staff of the LURE laboratory for the support of this work. JP wishes to thank for the partial support of this work from the Laboratoire de Réactivité et de Chimie des Solides, Université de Picardie. The research described in this publication was supported in part by the International Science Foundation, Grants N LF8000 and LJ8100.

5. REFERENCES

1. C. Genin, A. Driouiche, B.Gérard and M.Figlarz, "Hydrogen bronzes of new oxides of the WO₃-MoO₃ system with hexagonal, pyrochlore and ReO₃-type structures," *Solid State Ionics* **53&56**, 315-323 (1992).
2. C.G. Grangvist, *Handbook of Inorganic Electrochromic Materials*, Elsevier Science, Amsterdam, 1995.
3. B.O. Loopstra and H.M. Rietveld, "Further refinement of the structure of WO₃," *Acta Crystallogr. B* **25**, 1420-1421 (1966).
4. P.G. Dickens and R.J. Hurditch, *Electronic Properties of Hydrogen Tungsten Bronzes H_xWO₃*, in the Chemistry of Extended Defects in Non-Metallic Solids, North-Holland, Amsterdam, 1970.
5. A. Kuzmin, "EDA: EXAFS data analysis software package," *Physica B* **208&209**, 175-176 (1995).
6. A. Kuzmin and J. Purans, "X-ray absorption spectroscopy study of local structural changes in a-WO₃ under coloration," *J. Phys.: Condensed Matter* **5**, 2333-2340 (1993).
7. A. Kuzmin, J. Purans, J. Benfatto and C.R. Natoli, "X-ray-absorption study of rhenium L₃ and L₁ edges in ReO₃: Multiple-scattering approach," *Phys. Rev. B* **47**, 2480-2486 (1993).
8. A. Kuzmin and J. Purans, "X-ray absorption spectroscopy study of the local environment around tungsten and molybdenum ions in tungsten-phosphate and molybdenum-phosphate glasses," (in this Proceedings).
9. J. Oi, A. Kishimoto, T. Kudo and M. Hiratani, "Hexagonal tungsten trioxide obtained from peroxo-polytungstate and reversible lithium electro-intercalation into its framework," *J.Solid State Chem.* **96** 13-19 (1992).

Table 1. Best-fit values of distances R (in Å, ± 0.01 Å) and DW factors s^2 (in Å², $\pm 30\%$) for the first coordination shell of tungsten obtained by multi-shell fit of XAFS spectra (ϵ is the fitting error [5]). The XRD data from [1-4,9] are shown for comparison. $\Delta = \langle R \rangle_{\text{XRD}} - \langle R \rangle_{\text{XAFS}}$ (in Å) is the difference between average distances given by XRD and XAFS.

Compound	XAFS				XRD		Δ
	N	R (Å)	s^2	$\epsilon \times 10^{-4}$	N	$\langle R \rangle$	
c-ReO ₃	6	1.86	0.0031	25	6	1.87	0.01
c-WO ₃	6	1.89 ^a	0.013	19	6	1.85 ^b	-0.04
H _x (c-WO ₃)	6	1.89 ^a	0.015	33	6	1.87 ^b	-0.02
m-WO ₃	3	1.79	0.0032	14	3	1.79	0.00
	3	2.09	0.011		3	2.07	-0.02
m-WO ₃	2	1.77	0.0010	7	2	1.75	-0.02
	2	1.91	0.0084		2	1.90	-0.01
	2	2.15	0.0042		2	2.14	-0.01
H _x (m-WO ₃)	6	1.92 ^a	0.017	78	6	1.88 ^b	-0.04
H _x (m-WO ₃)	2	1.82	0.0017	27	4	1.87 ^b	0.05
	2	1.93	0.0048		2	1.88 ^b	-0.05
	2	2.10	0.0071				
h-WO ₃	4	1.82 ^a	0.084	74	4	1.89 ^b	0.07
	2	2.11	0.060		2	1.95 ^b	-0.16
h-WO ₃	2	1.78	0.0014	8	2		
	2	1.94	0.0078		2	1.95 ^b	0.01
	2	2.15	0.0080		2		
H _x (h-WO ₃)	4	1.84	0.0073	36	4		
	2	1.99	0.0176		2	1.89 ^b	-0.10
H _x (h-WO ₃)	2	1.81	0.0030	8	2		
	2	1.89	0.0057		2	1.89 ^b	0.00
	2	2.04	0.0130		2		

^a These best fits were done using a cumulants approach.

^b These distances were calculated using XRD cell parameters assuming linear chain W-O-W so that $\langle R \rangle = a/2$.

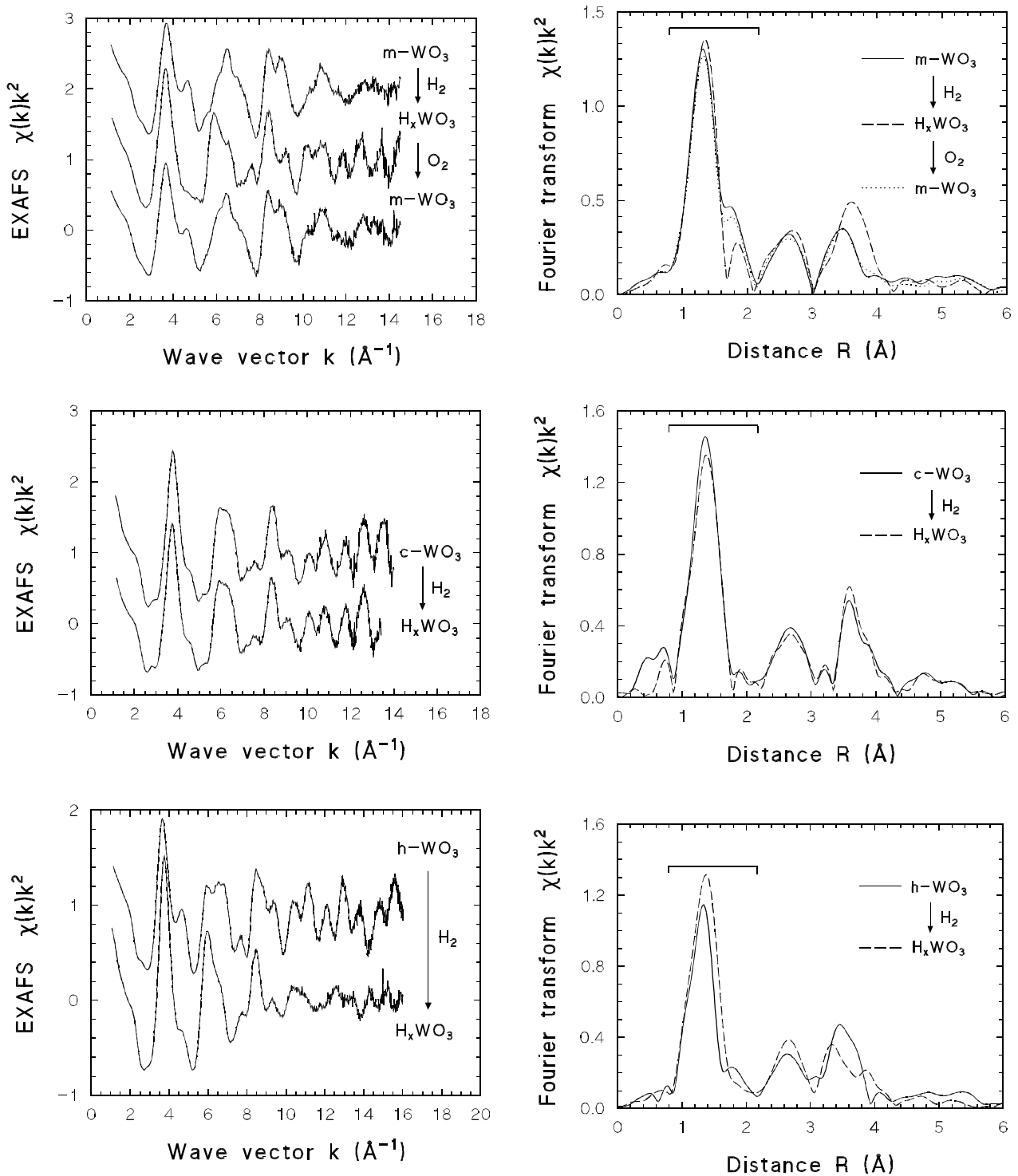


Fig. 1. Experimental XAFS spectra measured at the W L₃-edge in m-WO₃, c-WO₃ and h-WO₃ before and after hydrogen intercalation (left-hand panels) and their Fourier transforms (right-hand panels). For m-WO₃, also the signal after hydrogen deintercalation is presented.

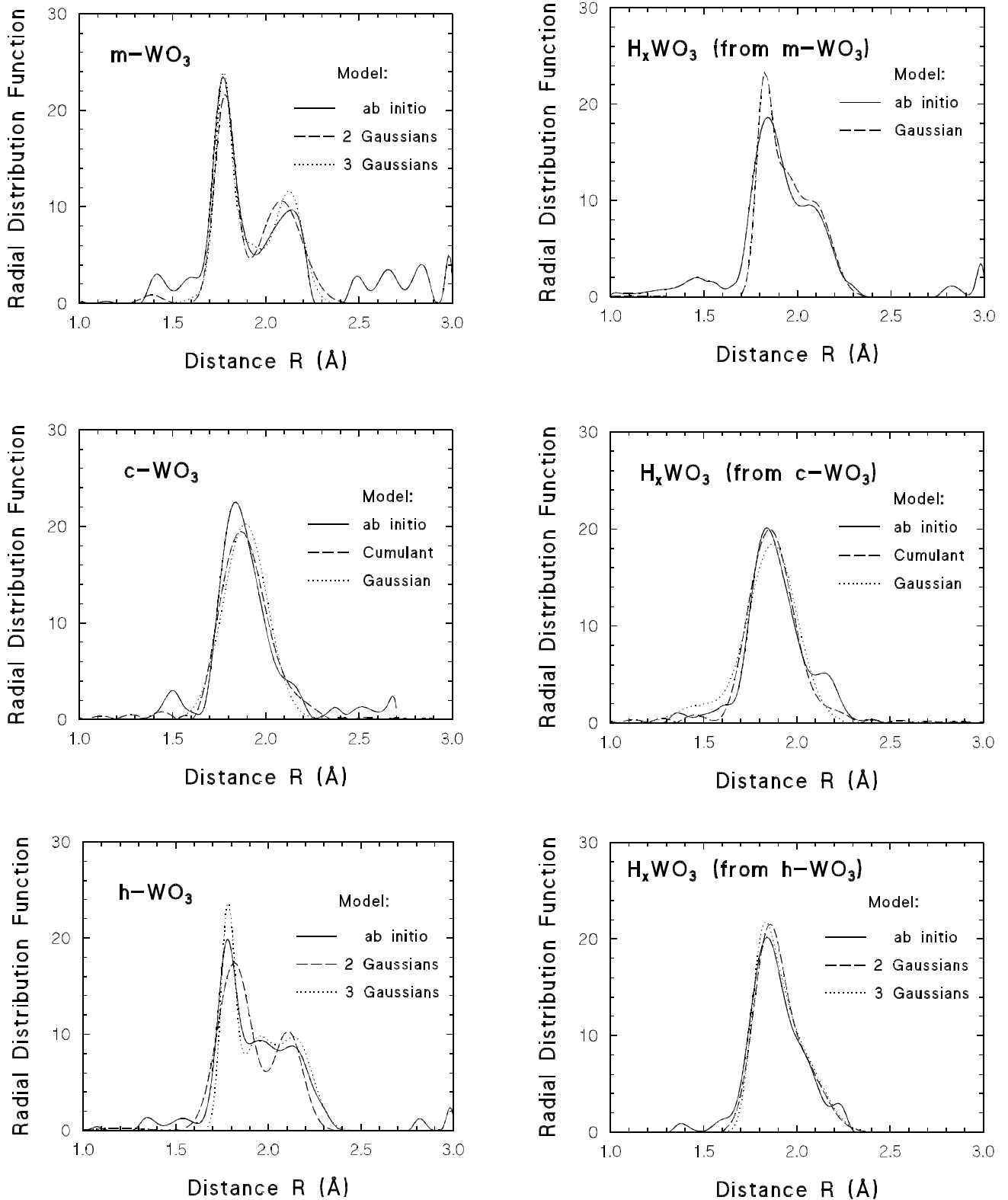


Fig. 2. The RDF's for the first shell of tungsten in tungsten oxides before (left-hand panels) and after hydrogen intercalation (right-hand panels). The RDF's were obtained within three approaches: (1) cumulant model; (2) multi-shell Gaussian model and (3) model-independent ("ab initio") model [5].